ISIJ International, Vol. 49 (2009), No. 1, pp. 132–138

The Influence of Austempering Temperature on the Wear Resistance of Ductile Iron under Two Different Tribosystems

Sebastian LAINO, Hugo R. ORTIZ and Ricardo C. DOMMARCO

Tribology Group, School of Engineering, Universidad Nacional de Mar del Plata, Metallurgy Department, INTEMA–CONICET, Av. J. B. Justo 4302, B7608FDQ Mar del Plata, Argentina. E-mail: slaino@fi.mdp.edu.ar

(*Received on September 2, 2008; accepted on October 3, 2008*)

This paper reports the results obtained in a research conducted to evaluate austempered ductile iron (ADI) as a wear resistant material for the production of machine parts processed at intermediate and high austempering temperatures (Ta). Severe abrasion in actual service performance trials and low stress abrasion laboratory tests (ASTM G-65) were carried out along with microstructural characterization by optical microscopy and X-ray diffraction. The results derived show that ADI yields excellent abrasion resistance under the operating conditions resulting from the field tests when Ta is raised. Nevertheless, ADI show an opposite trend under the low stress abrasion conditions imposed by the dry sand/rubber wheel abrasion apparatus (ASTM G-65). The presence of a metastable and ductile ausferrite phase (reacted and unreacted austenite+ferrite) in ADI microstructure appears to be the most relevant factor influencing the performance observed. In addition to a high deformation capability detected at the wear surfaces, an austenite to martensite transformation took place as determined by X-ray diffraction. These two factors combined make the ausferritic microstructure overcome hardness reduction when the austempering temperature is raised, improving or sustaining the resistance to severe abrasive wear but, at the same time, increasing impact toughness.

KEY WORDS: abrasion; ductile iron; austempering; microstructure; hardness.

1. Introduction

The abrasive wear mechanism occurs when the surface asperities of one body contact and indent the surface of a softer second body in relative motion, removing material by micro-cutting and/or micro-ploughing, and thereby creating a scratch. The abrasive wear is of particular concern in industrial areas such as mining, agriculture, earth moving, *etc.*

The magnitude of the damage caused by abrasive wear depends on several factors, such as: contact pressure, velocity, temperature, humidity, the wearing to abrasive material hardness ratio, the abrasive geometry, *etc.* Owing to the large number of possible combinations of influential factors, abrasive wear is frequently classified according to the conditions under which wear takes place.[1)] Among classifications, two- and three-body abrasive wear are probably the most frequently employed. Low- and high-stress abrasion classifications are common practice too.

One of the most important factors affecting abrasion resistance is the microstructure of the material being abraded, generally characterized by its hardness when this wear mechanism is of main concern. The amount of material removed by abrasion depends on the volume of the individual scratches, and hence on hardness.[2)] The higher the hardness the shallower the scratch is, thus promoting the common and often valid assumption that abrasion resistance can be optimized by increasing material hardness. This was demonstrated to be true for pure metals.[3)] Still the rate at which the abrasion resistance increases with hardness is lower for alloys, either with matrices strengthened by heat treatment, deformation or reinforcing particles.[4)]

• **Abrasive Wear Resistance of Austempered Ductile Iron.** ADI provides engineers with the distinctive benefits of conventional ductile iron plus enhanced mechanical properties thanks to a particular microstructure called ausferrite obtained by austempering. Such microstructure consists of graphite nodules immersed in a matrix of ferrite needles or feathers (depending on heat treatment temperature) and retained austenite.

Previous research characterized the mechanical properties of ADI over a range of austempering temperatures (Ta=220–360°C).[5,6)] Some authors call structures obtained bellow Ta=280–300°C austempered bainitic ductile iron or ABDI. The results show that abrasion resistance increases as austempering temperature decreases, also leading to a higher hardness. Even in laboratory and field tests on soil plowing tools[7–10)] ADI wear resistance was observed to increase as austempering temperature decreased. Based on the observation of wear scars shape, it is clear that all these experiments were conducted under low stress abrasion.

Laboratory tests have demonstrated that ADI highest wear resistance was obtained at intermediate austempering temperatures grades.[11)] It was also reported[12)] that the abra-

sive wear resistance (ASTM G 65) and hardness of permanent molded ADI castings could be increased by raising the amount of retained austenite upon Si content reduction.

When tested in a pin-on-disk abrasion test,[13] frequently regarded as a high stress test, ADI has yielded higher abrasion resistance than Q&T ductile iron, Q&T steels and austempered steels of similar hardness. This behavior was attributed mainly to the presence of austenite and to its subsequent strain-induced transformation to martensite.

Other studies have been undertaken to evaluate the potential use of ductile iron in earth moving equipment parts with a single pass grooving pendulum.[14] It was demonstrated that for constant austempering temperature, the wear resistance reached its peak at the austempering time promoting the highest austenite content. As the austempering temperature decreased, both the wear resistance and the hardness increased, while austenite levels decreased.[15] Nevertheless, it has also been reported that the wear behavior of ADI depends on the retained austenite content, though whether it will be beneficial or not, depends on the tribosystem.[16]

In a previous work[17] the authors reported that, unlike the common understanding, as austempering temperature increases and hardness decreases, the resistance to abrasion of ADI bucket tips increases, reaching higher values than those obtained for Q&T steel used as reference material. This behavior was detected for high stress abrasion as determined by the wear scar analysis.

The high abrasion resistance of ADI has been related to its unique microstructure. ADI matrix microstructure may contain up to 35–40% austenite that transforms into martensite in service when abraded.[13,17,18] The austenite features good ductility, and the martensitic transformation itself is accompanied by some plastic deformation, which involves extra energy consumption in order to cut and remove a microchip during abrasion.

There is no evidence in the literature of a clear relationship between ADI's microstructure and wear performance. This could be attributed to the lack of a detailed description of the abrasive tribosystems,[1] taking them as part of the same category, while, in fact, they are very different.

Therefore, the objective of the present work was to evaluate the abrasion resistance of ADI obtained at different austempering temperatures under two different abrasive severities. Wear resistance was assessed in field tests using ADI tips mounted on a wheel loader bucket as well as with laboratory wear tests in a dry sand-rubber wheel abrasion test to compare the material performance under two different tribosystems. Considering prior results which yielded an increase in abrasion resistance as hardness decreased, the present study determines the limit for the austempering temperature rise at which the abrasion resistance begins to decrease in field tests. Apart from the detailed microstructural characterization by optical microscopy and X-ray diffraction, a wear scars analysis was conducted.

2. Experimental Procedure

2.1. Samples Production

The ductile iron tips and the Y-blocks (ASTM A 395) were made from the same batch of cast iron produced in a cupola furnace. Inoculation and nodulization were made with FeSi and FeSiMg, respectively. Laboratory test samples were machined from the Y-blocks and then austempered together with the tips by austenitizing at $T\gamma = 920°C$ during $t\gamma = 120$ min in a muffle, and then soaking in a salt bath for the isothermal transformation at $Ta = 280–360°C$ during $ta = 120$ min. **Table 1** lists the austempering temperatures used and the identification given to the samples.

Table 1. Identification and heat treatment parameters of the different tip groups and laboratory samples evaluated.

Identification	Austenitizing Temperature - Tγ	Austempering Temperature – Ta
ADI280 (ref.mat.)	920 °C	280 °C
ADI300	920 °C	300 °C
ADI320	920 °C	320 °C
ADI340	920 °C	340 °C
ADI360	920 °C	360 °C

2.2. Microstructural Examination

The chemical composition was determined by means of a Baird Spark Emission Optic Spectrograph with DV6 excitation source. The metallographic samples preparation was carried out as prescribed by standard polishing techniques and etching with 2% Nital.

X-ray analyses were performed to determine the retained austenite (γ_{ret}) content by using a Phillips goniometer with a Co-Kα X-ray tube operating at 40 kV/30 mA. The scan ranged from 48 to 54 degrees of 2θ, where the austenite (γ-111) and ferrite (α-110) peaks are located, with a data collection velocity of 1°/min. The retained austenite was measured on non-deformed surfaces obtained by classical metallographic preparation, and then etched at a depth of up to ~40 mm, by using HNO_3 20% in order to eliminate deformed layers. The retained austenite content was also measured over worn surfaces at the end of the tip life.

2.3. Mechanical Tests

All samples for tensile and laboratory wear tests were machined from the Y-blocks. The Brinell hardness of the samples was measured by using a bench tester with a 2.5 mm tungsten carbide ball and 187.5 kg load ($HBW_{2.5/187.5}$). Tensile tests were performed in accordance with the ASTM E 8 standard. The reported values are the average of three determinations.

The samples abrasive wear resistance, either pertaining to the laboratory or the field tests, was evaluated by means of the Relative Wear Resistance index—*E*. Such index was calculated as the relation between the volume loss experienced by a reference material with respect to ADI sample, in agreement with Eq. (1).

$$E = \frac{\Delta V_R}{\Delta V_S} \quad \text{.....(1)}$$

Where: E = Relative wear resistance
ΔV_R = Average Reference volume difference
ΔV_S = Average Sample volume difference

The laboratory abrasion tests were performed under the ASTM G 65 standard, and the E values were obtained by using SAE 1010 as reference material. The test uses

rounded quartzitic sand of about 0.2 mm in diameter. The weight of the samples was measured by a 0.1 mg precision scale, and then converted to volume loss.

The reference and sample tips used in the field tests were mounted on a 2 m^3 bucket of a 110 HP wheel loader. The loader was involved in handling and loading quartzitic gravel with a compression resistance of 1 000 kg/cm^2 and a 10–30 mm size range. Eight tips were mounted on the bucket, six of them made of the experimental iron and the remaining two of the reference iron, in this case the ADI280 variant. Tips were removed periodically during service, weighed and then re-placed in the same position in the bucket. Depending on their position in the bucket, the tips suffer different wear rates. Between them, the two at the center of the bucket have similar wear rates, therefore, the ΔV_R and ΔV_S values were calculated by the weight lost by the reference and sample tips located in these positions, whilst the remaining were used for reference purposes only. Two sets of tips were evaluated in the field for each austempering temperature variant. Weight differences were measured by an electronic scale with a 5 g sensitivity.

The wear scars were analyzed by optical macro and microscopy and the individual scratches, with a profile meter Talysurf Surtronic 3+.

3. Results and Discusion

3.1. Chemical Composition and Microstructural Characterization

The chemical composition of the alloy is listed in **Table 2**. The melt includes low amounts of Cu and Mo added to provide this application with sufficient austemperability. The equivalent carbon (EC=4.34) was almost eutectic so as to avoid primary nodules formation.

The alloy austemperability was evaluated by microstructural analysis and hardness measurements for the ADI360 variant. A tip was cut along its longitudinal axis and the results demonstrate that the microstructure was fully ausferritic both close to the surface, (**Fig. 1**(a)) with a hardness of 317 $HBW_{2.5/187.5}$ and at the center of the tip, (Fig. 1(b)) with a hardness of 306 $HBW_{2.5/187.5}$. No evidence of pearlite precipitation was detected, thus confirming that the austemperability given by the alloying elements was enough for the tip size. The decrease in hardness to the center of the tip is normal and originated by the cooling rate gradient. As for the other ADI variants, the higher cooling rates favor pearlitic structures avoidance.

The X-ray diffraction diagrams for samples of ADI280 to ADI340, superimposed on the same plot in **Fig. 2**, illustrate austenite (γ-111) and ferrite (α-110) peaks. The results show that the amount of retained austenite (γ_{ret}), indicated by the height of the γ-111 peak, increases as the austempering temperature does too. **Table 3** lists the retained austenite content measured from the X-ray diffraction diagrams. The amount of retained austenite rises from 13.0% at Ta=280°C up to 41% at Ta=340°C. It is considered that, at low Ta, ferrite needles grow rapidly within the austenite due to the high driving force. Yet at the same time, carbon diffusion is low and austenite saturates in carbon, thus precipitating ε carbides. The reaction proceeds continuously and the resulting amount of γ_{ret} is low.[19] On

Table 2. Chemical composition of the heat used for tips and Y-blocks.

Element	C	Si	Mn	S	P	Mg	Cu	Mo	EC
Sample	3.29	2.58	0.31	0.032	0.046	0.08	0.72	0.19	4.34

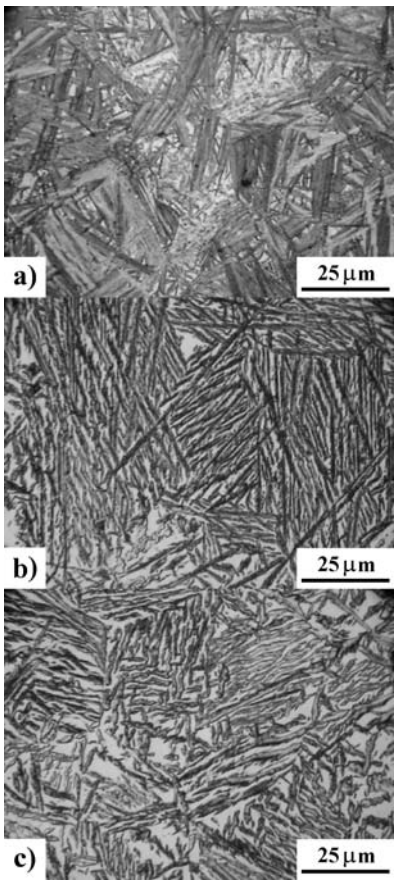

Fig. 1. Ausferritic microstructures of ADI tips, (a) austempered at 280°C, (b) austempered at 360°C, close to the surface, (c) austempered at 360°C, at center of thickest section of the tip. Nital 2%.

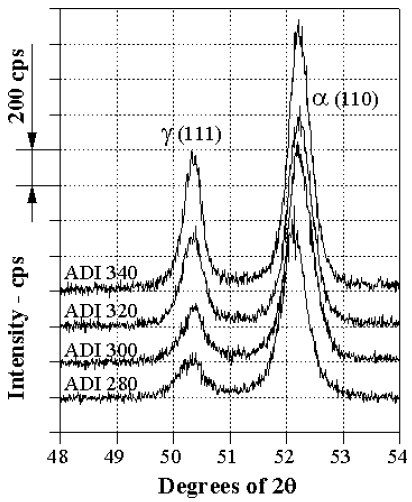

Fig. 2. X-ray diffraction patterns for the γ_{ret} measurement, obtained for unworn surfaces. Mo-Kα radiation, 50 kV, 30 mA.

Table 3. Retained austenite, tensile properties and hardness for the different ADI variants.

Identif.	Ret. Aust. γ_{ret} - %	YS - MPa	UTS - MPa	Hardness $HBW_{2.5/187.5}$
ADI280	13.0	1250	1490	482 (4)
ADI300	16.0	1170	1440	444 (6)
ADI320	35.0	1200	1340	409 (5)
ADI340	41.0	1100	1190	368 (5)
ADI360				317 (3)

σ_n values in brackets

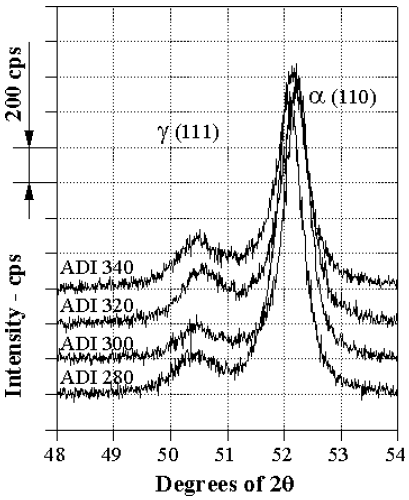

Fig. 3. X-ray diffraction patterns for tips worn surfaces, showing plastic deformation and austenite to martensite transformation. Mo-Kα radiation, 50 kV, 30 mA.

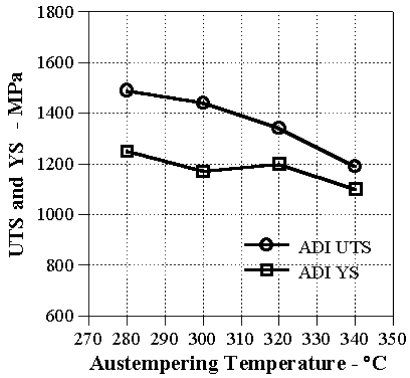

Fig. 4. Elastic limit and ultimate tensile strength for the different ADI variants.

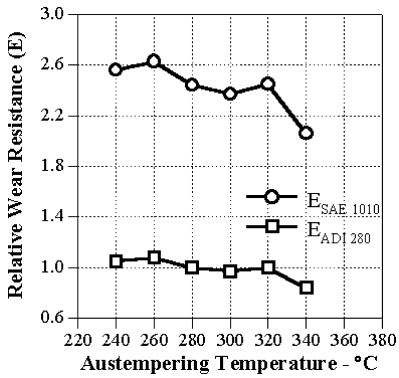

Fig. 5. Relative wear resistance of the different ADI variants tested at the laboratory by the dry-sand rubber wheel abrasion test (ASTM G 65).

the other hand, when Ta is high the driving force is lower, though carbon diffusion is higher. Hence during the growing process of ferrite, carbon is rejected and piles up ahead of the moving interface and then diffuses into the surrounding austenite enriching this phase up to ~2% C, and then ferrite growth is arrested.[19] With such carbon content in the austenite, M_s temperature decreases and, therefore, a larger amount of γ_{ret} is obtained.

Figure 3 depicts the X-ray diffraction diagrams obtained for ADI tips worn surfaces. The pattern of peaks shows noticeable changes as a result of the wear process. Compared to the unworn specimens, worn samples show wider and shorter peaks. The decrease in intensity of the $\gamma(111)$ is particularly marked, due to the austenite to martensite transformation.

3.2. Mechanical Properties

• **Tensile Tests.** The results of the tensile tests performed are listed in Table 3, with the reported values obtained as the average of three samples. The tensile properties were evaluated for the ADI variants austempered from Ta=280°C up to 340°C, rendering values for the ultimate tensile strength (UTS) from 1 490 MPa down to 1 190 MPa, respectively (**Fig. 4**). This figure also shows the values for yield strength (YS), ranging from 1 250 MPa for Ta=280°C to 1 100 MPa for Ta=340°C. These results indicate classical trends and levels for ADI strength with respect to the austempering temperature, as dictated by the ASTM A 897 standard.

Table 3 lists the results of hardness readings corresponding to the laboratory samples obtained from the Y-blocks, with values ranging from 368 up to 482 $HBW_{2.5/187.5}$ for Ta=340 and 280°C, respectively.

• **Laboratory Wear Tests.** Using the volume loss values obtained from the laboratory wear tests, the Relative Wear Resistance index "*E*" was obtained for two reference materials: SAE 1010 with a density of $\delta \approx 7.7$ g/cm^3, and ADI280 ductile iron with a density value of $\delta \approx 7.1$ g/cm^3.

Figure 5 shows the relative wear resistance of ADI as a function of austempering temperature. The results were obtained from the dry sand/rubber wheel abrasion tests, and *E* values are given for the two reference materials used. The abrasion resistance was higher for the lower austempering temperatures ($E_{SAE1010}$=2.4@Ta=280°C), and tended to decrease for the highest austempering temperatures evaluated ($E_{SAE1010}$=2.0@Ta=340°C). Previous results[17] obtained for Ta=240, 260, and also 280°C as in the present paper, were also included in Fig. 5 in order to analyze the trend over a wider austempering temperature range, even when sometimes these low austempering temperatures are not considered to promote pure ADI structures. Figure 5 also shows the relative wear resistance with ADI280 as reference material (E_{ADI280}).

• **Tips Service Assessment.** **Figure 6** shows the *E* *versus* service life curves obtained for the field tests carried out by mounting the tip samples on a wheel loader bucket. In such same figure (Fig. 6), the *E* values attained for the present work are compared to those obtained in a previous work for lower austempering temperatures, *i.e.* at Ta=240, 260 and 280°C. All tips made of ADI300 to ADI360

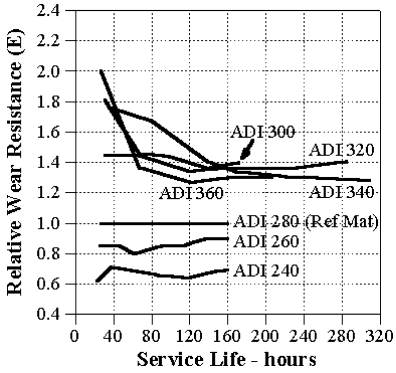

Fig. 6. Relative wear resistance of ADI variants obtained by testing the tips on the wheel loader. Reference material ADI280.

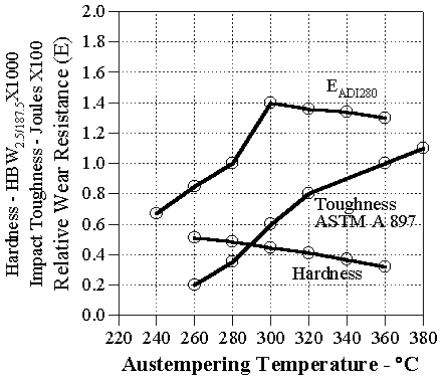

Fig. 7. Field tests Relative wear resistance, hardness and impact toughness according to ASTM A 897, *versus* austempering temperature.

yielded consistently higher E with respect to the reference material ADI280. **Figure 7** shows the value of E as a function of austempering temperature at 160 h of service life, *i.e.* once the different curves seem to be stabilized after the initial stage. As opposed to laboratory tests observations, in field tests, *i.e.* under more severe abrasive conditions than those in the laboratory, results reveal that the relative wear resistance increases as ADI austempering temperature does. E increases markedly up to $E=1.4$@Ta=300°C, and then there is a slight decrease in the wear resistance till $E=1.3$@Ta=360°C. Figure 7 also shows that hardness decreases as the austempering temperature increases, as expected. Noticeably, the trend of E variation for the field tests opposes that observed in laboratory wear tests.

These results show that for the service conditions investigated, the greater abrasion resistance is obtained for ADI austempered at temperatures between 300 and 360°C, and as it was proposed for the present investigation the highest abrasion resistance was found at Ta=300°C. It should be noted that in a previous research[17] the ADI280 variant showed an abrasion resistance $E>1.35$ with respect to a quenched and tempered steel (0.31% C, 0.5% Cr, 0.13% Mo) with a hardness of 50 HRC.

- **Wear Scars Analysis and Degree of Wear.** The different abrasive conditions between laboratory and field tests lead to different wear scars. **Figures 8**(a) and 8(b) show the surface of and ADI280 laboratory test and field test samples, respectively. The scratches of the laboratory test sample are smaller, parallel and shallow, being difficult to observe even by tilting at the SEM. Scratches on the field test specimens, conversely, are much larger (about an order of magnitude wider), and feature plastic flow by the formation of lips at the scratches edge. This clearly indicates that the material was subjected to more severe plastic deformation in the field tests.

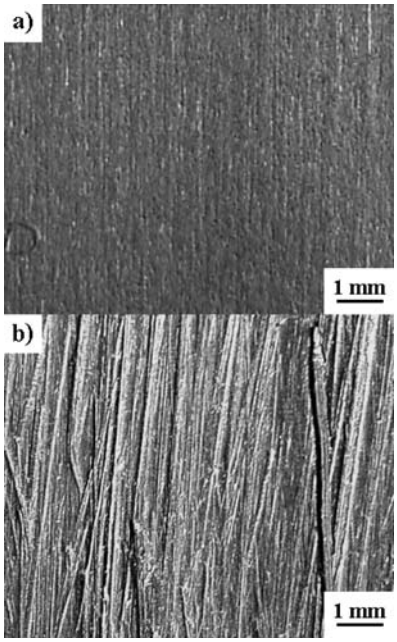

Fig. 8. Wear scars of an ADI 280 sample, (a) laboratory test, (b) field test.

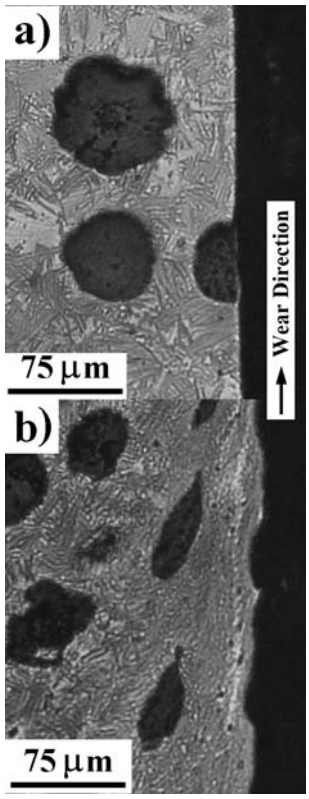

Fig. 9. ADI 280 microstructure under the wear scars, (a) laboratory test, (b) field test.

The extent of plastic deformation under the surface was analyzed. **Figures 9**(a) and 9(b) depict the microstructure

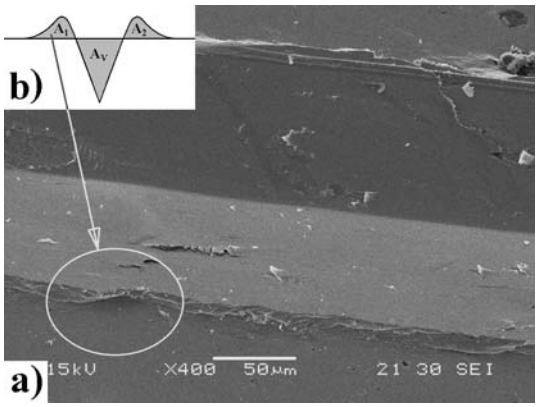

Fig. 10. (a) Scheme of a scratch section, (b) a 5 kg Vickers scratch on ADI 320 sample with detail showing build up at the edge scratch.

under the wear scars of ADI 280 laboratory and field test specimens, respectively. As shown by the change in the shape of the graphite spheroids and the matrix, the layer of material affected by plastic deformation was thinner than 5 μm for the laboratory test sample (Fig. 9(a)) while, a severely deformed layer reaching a depth of nearly 100 μm was observed at the surface of the field test specimens.

Scratch Test: A typical scratch process can be assumed to be produced by a conical tip with a section (A_v). During the process, a portion of material is displaced to the sides of the scratch (A_1, A_2) by plastic deformation, **Fig. 10**(a). The f_{ab} factor or "degree of wear" (Eq. (2)) is the relation between the material being cut away or lost by the asperity action ($A_v-(A_1+A_2)$) with respect to the section of the scratch (A_v). The number so derived accounts for the balance between the ability of the material to accommodate itself by plastic deformation (rather than being cut away like a chip) and its hardness or resistance to penetration.[20,21] The greater the f_{ab}, the larger the wear rate is.

$$f_{ab}=(A_v-(A_1+A_2))/A_v \quad \text{.....(2)}$$

Figure 10(b) shows a 5 kg scratch obtained with a Vickers pyramid with the scratch parallel to the indenter diagonal. The detail in Fig. 10(a) shows the material build up at the edges of the scratch. For scratches made with 1 kg load, A_v depths of about ~6.5 and ~7.5 μm and A_1, A_2 heights of ~4.0 and ~5.0 μm were measured for ADI280 and ADI320, respectively. These values resulted in similar degree of wear ($f_{ab}\approx 0.4$) for both ADI variants, also demonstrating by the scratch test that the lower hardness level of ADI320 does not necessarily correspond to a lower abrasion resistance.

3.3. Discussion

By replicating previous results and extending the analysis to higher and wider austempering temperature range, this study proved that ADI's response to abrasive wear strongly depends on the tribosystem. Two different wear tests were used to this end, the dry sand rubber wheel abrasion test in the lab and a wheel loader in the field. The different abrasiveness of both tests was evaluated and corroborated by the wear scars analysis.

The laboratory tests wear scar show a relatively smooth surface profile with a shallow deformation layer. Even though the strain-induced austenite to martensite transformation should occur, as is the case for ADI tips, this is difficult to observe[17] with the diffraction technique used. This is due to the relatively deep measurement volume with respect to the thin deformed layer (shallower than 5 μm), since 90% of the collected data comes from the first 15–20 μm.

The concepts of "degree of penetration (Dp)" and "wear mode"[22] predict that for the rounded abrasive particles employed, with an average diameter of ~200 μm, and a hardness of 400 HBW for the abraded material, the load over each particle should be higher than 0.5 kg for micro-cutting abrasion. Therefore, micro-ploughing and hence micro-fatigue are the most probable micromechanism for the laboratory tests. Under these loading conditions usually termed low stress, ADI abrasion resistance has a clear trend to increase with hardness.

On the other side, field tests have shown more severity than laboratory tests, as seen by the wear scars and the depth of the deformed layer. Even though the ductility of ADI in tension was relatively low as a whole because of graphite nodules presence, the matrix was able to accommodate high degrees of deformation. This is possible for ADI at the scale at which the abrasion scratches take place, thanks to the ausferrite ductility as shown in Figs. 8 and 9. This promotes the matrix strengthening as well as the austenite to martensite transformation as evidenced in Fig. 3. The plasticity of the higher austempering temperatures also proved to be beneficial according to the f_{ab} analysis on ADI280 (482 HBW) and ADI320 (409 HBW) variants, whose degree of wear ($f_{ab}\approx$0,4) is similar, though their field abrasion resistance values are of $E_{ADI280}=1.0$ and $E_{ADI280}\approx 1.4$, respectively. Thus the lower hardness level of ADI320 does not necessarily correspond to a lower abrasion resistance as it is usually thought. Similar results were obtained in previous research[23] wherein f_{ab} factors for ADI and Q&T ductile iron were compared.

Under the loading conditions of the field tests, ADI abrasion resistance increases as hardness decreases up to Ta~300–320°C, and then it tends to decrease at a low rate up to the temperature evaluated in this study, Ta=360°C. It should be noted that even when field abrasion resistance slowly decreases over Ta=300°C, at the same time according to the ASTM A 897 standard, an increase in impact toughness from approximately 60 to 110 Joules is concurrently expected. This shows that even with a bit lower abrasion resistance, higher austempering temperatures could be an excellent choice for many applications also involving impact loads. Similar results were presented by Zimba *et al.*[24]

4. Conclusions

The results of the present study have shown that ADI's response to abrasive wear depends on the tribosystems, yielding significant differences between laboratory (low stress) and field (high stress) abrasion tests.

Field tests carried out on bucket tips made of ADI demonstrated that the abrasion wear resistance of high austempering temperature ADI is greater than that measured on harder grades of ADI, austempered at lower tem-

peratures. The decrease in hardness is compensated by an increased ductility allowing ADI matrix to accommodate.

It was determined that under this testing conditions abrasion resistance was highest at about Ta≈300°C, and then has a small decrease up to Ta=360°C. An interesting feature accompanying this response to wear, is an increase in impact toughness, as predicted by the ASTM A 897 standard.

The behavior of ADI observed for the dry sand/rubber wheel abrasion laboratory tests reflected an opposite trend, increasing wear resistance as hardness increased too. Far from invalidating the use of this laboratory test, these results show that its use should be carefully evaluated and applied to rank candidate materials for a given application and used for those tribosystems with similar characteristics, for example the wear scars.

Acknowledgments

The authors whish to thank the authorities of the Ente Municipal de Vialidad Servicios Urbanos y Gestión Ambiental (Gral. Pueyrredón county, Buenos Aires Province) for providing the industrial equipment for the trial tests.

REFERENCES

1) J. D. Gates: *Wear*, **214** (1994), 139.
2) J. F. Archard: *J. Appl. Phys.*, **24** (1960), 981.
3) M. M. Kruschov and M. A. Babichev: *Friction and Wear in Machinery*, **12** (1958), 1.
4) K. H. Zum Gahr: *Tribol. Int.*, **31** (1998), 587.
5) R. C. Dommarco, H. A. Dall'O and H. R. Ortiz: Proc. Jornadas Metalúrgicas S.A.M., Sociedad Argentina de Metales, Buenos Aires, (1991), 99.
6) H. A. Dall'O, H. R. Ortiz and R. C. Dommarco: Proc. Jornadas Tribológicas de la Rca. Argentina Tribos '94, Centro Argentino de Tribología, Buenos Aires, (1994).
7) J. García, J. Sikora and H. Dall'O: Proc. Jornadas Tribológicas de la Rca. Argentina Tribos '94, Centro Argentino de Tribología, Buenos Aires, (1994).
8) J. Sikora, J. Capurro, J. García and H. Dall'O: Proc. Jornadas Metalúrgicas S.A.M., Sociedad Argentina de Metales, Buenos Aires, (1994), 137.
9) H. Farina and J. Sikora: Proc. Jornadas Metalúrgicas S.A.M. '98 and IBEROMET V, Sociedad Argentina de Metales, Rosario, Argentina, (1998), 97.
10) J. Capurro, M. Nolasco and J. Sikora: Proc. IV Congreso Argentino y II Internacional de Ingeniería Rural, Neuquén, Argentina, (1996), 319.
11) M. Martinez Gamba, J. García, H. Dall'O and J. Sikora: Proc. Jornadas Metalúrgicas S.A.M., Sociedad Argentina de Metales, Bahía Blanca, Argentina, (1994), 133.
12) S. Seetharamu, P. Sampathkumaran, K. Kumar, K. Narashima Murthy and P. Martin Jebraj: *Wear*, **167** (1993), 1.
13) Q. Luo, J. Xie and Y. Song: *Wear*, **184** (1995), 1.
14) J. M. Velez and A. P. Tschiptschin: Proc. 50° Congreso Anual da A.B.M., Asociacion Brasilera de Metales, Brasil, 2, (1995), 1.
15) J. M. Velez: PhD Thesis, Escola Politécnica, Universidade de Sao Paulo, Sao Paulo, Brasil, (1997), 226.
16) W. S. Zhou, D. Q. Zhou and S. K. Meng: *Cast Metals*, **6** (1993) No. 2, 69.
17) R. Dommarco, I. Galarreta, H. Ortíz, P. David and G. Maglieri: *Wear*, **249** (2001), 100.
18) S. Shepperson and C. Allen: *Wear*, **121** (1988), 271.
19) R. Elliot: Cast Iron Technology, Pub. Butterworths & Co., London, (1988), 126.
20) K. H. Zum Gahr: Microstructures and Wear of Materials, Tribology Series 10, Pub. Elsevier, Amsterdam, (1987).
21) K. H. Zum Gahr: *Wear*, **124** (1988), 87.
22) K. Hokkirigawa and K. Kato: *Tribol. Int.*, **21** (1988), 51.
23) R. Dommarco, M. Sousa and J. Sikora: *Wear*, **257** (2004), 1185.
24) J. Zimba, D. J. Simbi and E. Navarra: *Cem. Concr. Compos.*, **25** (2003), 643.